Modelling and Simulation of Micro-electro-Mechanical Systems for Energy Harvesting of Random Mechanical Vibrations

Modelling and simulation of micro-electro-mechanical systems for energy harvesting of random mechanical vibrations

Kailing Song[1,2] and Michele Bonnin[2]

[1] IUSS, University School for Advanced Studies, Pavia, Italy,
kailing.song@polito.it
[2] Department of Electronics and Telecommunication
Politecnico di Torino, Turin, Italy
michele.bonnin@polito.it

Abstract. We consider the problem of modelling and analyze nonlinear piezoelectric energy harvesters for ambient mechanical vibrations. The equations of motion are derived from the mechanical properties, the characterization of piezoelectric materials, and the circuit description of the electrical load. For random ambient vibrations, modelled as white Gaussian noise, the performances are analyzed through Monte-Carlo simulations. Recently proposed solutions inspired by circuit theory, aimed at improving the power performances of energy harvesters are tested. Our results show that circuit theory inspired solutions, permit to design energy harvesters with significant improved performances, also in the case of random vibrations.

Keywords: Energy harvesting, micro-electro-mechanical systems, random vibrations, nonlinear dynamical systems, circuit theory, noise, stochastic processes, stochastic differential equations.

1 Introduction

Over the past two decades, network technologies have become an integral part of our daily life. Networks of computers, routers, printers, mobile phones, and smart household appliances, that are wireless connected and exchange information through the Internet, have become common and are widespread. Wireless sensor and actuators networks (WSAN) are used both in work and home environments, to gather information about the surrounding ambient, and respond to the sensed events/data by performing appropriate actions. These networks may involve hundreds of nodes, made up by multi-domain systems, with both electrical and mechanical components.

Among the many challenges posed by network technologies, the problem of how supply power to the nodes is of fundamental importance. WSAN often include nodes that are remotely located and difficult to access, making battery replacement inconvenient. Furthermore, the progressive miniaturization of

electronic components discourage the use of batteries, that remain bulky and relatively heavy.

Systems capable of self-powering, collecting energy from the surrounding environment whenever available, would represent the ideal solution. Energy harvesting refers to a set of technical solutions, to realize micro-scale systems that are able to scavenge energy from ambient sources, like mechanical vibrations, thermal gradients, dispersed electromagnetic radiations, etc., and convert it into usable electrical power[1–5]. Kinetic energy, in the form of ambient mechanical vibrations, is particularly interesting, because it is widespread and it has relatively high power density. Kinetic energy from ambient mechanical vibrations can be converted into electrical power using different physical principles. In particular, piezoelectric materials offer a relatively cheap, easy to implement and reliable mechanism [6–9].

If the energy of ambient vibrations is concentrated at a single frequency, they can be modelled by a simple sinusoidal force [10]. Conversely, if vibrational energy is spread over a relative wide frequency interval, ambient vibrations are best described as a stochastic process. If the spectrum is reasonably flat, white Gaussian noise is a convenient approximation, because the theory of stochastic differential equation driven by white Gaussian noise is well developed. Alternatively, if the finite, non null noise correlation time is taken into account, a colored noise process can be used [11, 12].

The most important factor limiting the performances of a piezoelectric energy harvester is the impedance mismatch between the mechanical and the electrical parts. Impedance mismatch introduces a lag between current and voltage, that can be reduced introducing a proper reactive element in parallel with the load, a procedure known in circuit theory as power factor correction [10, 13].

In this work, we consider the problem of modelling a piezoelectric energy harvester subject to random mechanical vibrations, and its numerical analysis. The mathematical model is derived from the properties of the mechanical part, the constitutive equations for piezoelectric materials, and the circuit description of the electrical part. The model includes nonlinearities, which take into account nonlinear contributions in the mechanical stiffness of a cantilever beam. Ambient mechanical vibrations are modelled as a white Gaussian noise process. Consequently, the equations of motion are stochastic differential equations, that are solved using various numerical integration schemes. Inspired by recent work on the application of circuit theory to improve the efficiency of energy harvesting systems, we apply a power factor correction solution to the load [10, 14]. We evaluate the advantage offered by the modified load in terms of output average voltage and output average power. The numerical simulations shows that, even for the case of random mechanical vibrations, the application of power factor correction improves the performances by a significant amount.

2 Nonlinear piezoelectric energy harvesting: modelling

A piezoelectric energy harvester is a multi-domain system, with both mechanical and electrical parts. The mechanical structure is responsible for capturing the kinetic energy of parasitic mechanical vibrations. It is composed by a cantilever beam, fixed at one hand to a vibrating support, with an inertial mass at the opposite end. The cantilever beam is covered by a layer of piezoelectric material, that converts mechanical stress and strain into electrical power. A schematic representation of a piezoelectric cantilever beam energy harvester is shown in figure 1.

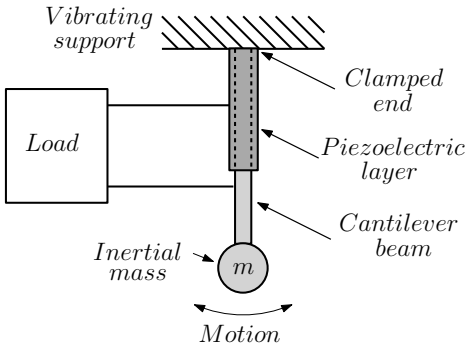

Fig. 1. Schematic representation of a piezoelectric cantilever beam energy harvester.

The equations of motion for the mechanical part are readily derived from classic mechanics

$$m\ddot{x} + \gamma\dot{x} + U'(x) + F_{pz} = F_m(t) \tag{1}$$

where m is the inertial mass, x is the displacement with respect to the equilibrium position, dots denote derivative with respect to time, γ is the damping coefficient, $U(x) = \frac{1}{2}k_1x^2 + \frac{1}{4}k_3x^4$ is a nonlinear elastic potential, and the $'$ denotes derivation with respect to the argument. For $k_3 = 0$ the harvester is linear, otherwise it is nonlinear. Finally, F_{pz} is the force exerted by the piezoelectric layer, and $F_m(t)$ is the external force modelling ambient vibrations.

The piezoelectric layer constitutes a mechanical-to-electrical power transducer. The governing equation for the transducer can be derived from the constitutive equations for a linear piezoelectric material [16]. Through spatial integration of the local variables, and neglecting the stiffness of the piezoelectric layer, the following relationships between mechanical and electrical variables are obtained

$$F_{pz} = \alpha\, e \tag{2}$$

$$q_{pz} = -\,\alpha\, x + C_{pz}\, e \tag{3}$$

where α is the electro-mechanical coupling (in N/V or As/m), C_{pz} is the electrical capacitance of the piezoelectric layer, and e is the output voltage.

The voltage is used to supply power to an electrical load, typically modelled as a resistor (see figure 2(b)). One of the most important factors limiting the harvested power, is the impedance mismatch between the electrical and the mechanical parts. In [10], it was proved, for the case a single frequency external excitation, that the harvested average power and the power efficiency can be significantly increased placing a reactive element in parallel with the resistive load, as shown in figure 2(a). The role of the inductive element, is to reduce the lag between the current and voltage induced by the capacitive reactance of the piezoelectric transducer, a method known in circuit theory as *power factor correction*.

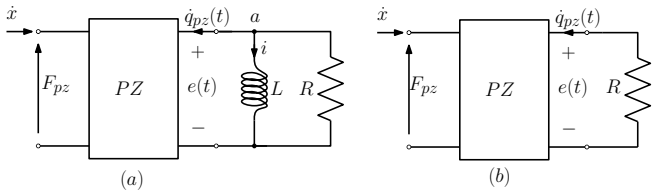

Fig. 2. Electrical load connected to the piezoelectric transducer PZ. Mechanical quantities are applied to the left port of the transducer and electrical quantities to the right. (a) Resistive-inductive load. (b) Resistive load.

For the resistive-inductive load of figure 2(a), application of Kirchhoff current law to the node a yields

$$\dot{q}_{pz} + i + Ge = 0 \tag{4}$$

where $G = 1/R$ is the load conductance. Introducing the linear momentum $y = \dot{x}/m$, and using the constitutive relationship for a linear inductor $e = L\,\dot{i}$, equations (1) and the time derivative of (3) give the state equations

$$\dot{x} = \frac{1}{m} y \tag{5a}$$

$$\dot{y} = -U'(x) - \frac{\gamma}{m} y - \alpha\, e + F_m(t) \tag{5b}$$

$$\dot{i} = \frac{1}{L} e \tag{5c}$$

$$\dot{e} = \frac{1}{C_{pz}} \left(\frac{\alpha}{m} y - i - G\, e \right) \tag{5d}$$

It is convenient to transform the electromechanical system into an equivalent electrical circuit. Equivalent means that the two systems are described by the same differential equations, although with different meaning of the state variables. Exploiting mechanical-to-electrical analogies, displacement x is replaced

by charge q, momentum y by flux linkage φ, mass m by inductance L_1, stiffness constants k_1, k_3 by the inverse of capacitance $1/C_1$, $1/C_3$, friction γ by resistance R_1, and force $F_m(t)$ by voltage $v_{in}(t)$.

The equivalent circuit for the electromechanical system, obtained after transformation of variables is shown in figure 3. The nonlinear stiffness of the beam is accounted for by a nonlinear charge controlled capacitor, with characteristic relationship $v_C(q) = \frac{1}{C_1}q + \frac{1}{C_3}q^3$. The piezoelectric transducer is modelled by an ideal transformer with turns ratio $1{:}n$, in parallel with a capacitor of capacitance C_{pz}. It is straightforward to derive the equations for the piezoelectric transducer model. Using the constitutive relationships for an ideal transformer, $v_s = nv_p$ and $i_s = -\frac{1}{n}i_p$, where v_p, v_s, i_p, i_s are the voltages and currents at the primary and secondary windings, respectively, and applying Kirchhoff current law to node c, we have

$$e = n\, v_p \tag{6}$$

$$\dot{q}_{pz} = -\frac{1}{n}\,\dot{q} + C_{pz}\dot{e} \tag{7}$$

that correspond to (2) and (3), where mechanical quantities have been replaced by their electrical analogous. It is worth mentioning that the turns ratio $n = \alpha^{-1}$ is an a-dimensional parameter. Rigorously speaking, n should have dimension V/N. However in mechanical-to-electrical analogies voltage and force are equivalent entities, known as "effort".

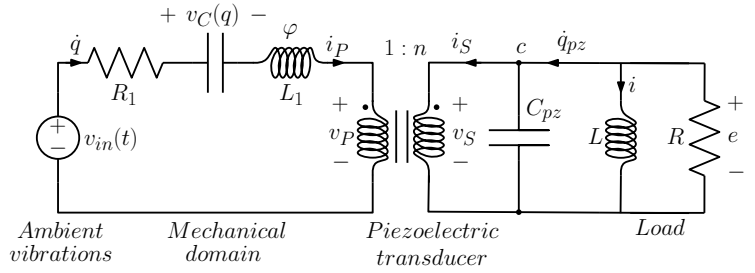

Fig. 3. Equivalent circuit for a piezoelectric nonlinear energy harvester with a resistive-inductive load.

To assess the advantage in harvested power offered by a resistive-inductive load in the case of random mechanical vibrations, we shall consider also a simple resistive load, as the one shown in figure 2(b). Introducing the linear momentum $y = \dot{x}/m$ in equation (1), taking derivatives with respect to time in (3) and using

the Ohm's law $\dot{q}_{pz} = -G\,e$ yields the state equations

$$\dot{x} = \frac{1}{m} y \tag{8a}$$

$$\dot{y} = -U'(x) - \frac{\gamma}{m} y - \alpha e + F_m(t) \tag{8b}$$

$$\dot{e} = \frac{1}{C_{pz}} \left(\frac{\alpha}{m} y - G\,e \right) \tag{8c}$$

The equivalent circuit for the energy harvester with resistive load is analogous to the one shown in figure 3, but without the inductor L in parallel with the resistor R.

3 Stochastic differential equations

Ambient mechanical vibrations are best described as stochastic processes. When the external force $F_m(t)$ is modelled as a random noise, the differential equations (5) or (8) become stochastic differential equations (SDEs).

Let $(\Omega, \mathcal{F}, P)$ be a probability space, where Ω is the sample space, $\mathcal{F} = (\mathcal{F}_t)_{t \geq 0}$ is a filtration, e.g. the σ-algebra of all the events, and P is a probability measure. Let $W_t = W(t)$ be a one dimensional Wiener process, characterized by $\langle W_t \rangle = 0$ (symbol $\langle \cdot \rangle$ denotes mean value), $cov(W_t, W_s) = \langle W_t W_s \rangle = \min(t, s)$ and $W_t \sim \mathcal{N}(0, t)$, where symbol $\sim$ means "distributed as", and $\mathcal{N}(0, t)$ denotes a normal distribution, centered at zero.

A d-dimensional system of SDEs driven by the one-dimensional Wiener process W_t is[3]

$$d\boldsymbol{X}_t = \boldsymbol{a}(\boldsymbol{X}_t)dt + \boldsymbol{B}(\boldsymbol{X}_t)dW_t \tag{9}$$

where $\boldsymbol{X}_t : \Omega \mapsto \mathbb{R}^d$ is a vector valued stochastic process, e.g. a vector of random variables parametrized by $t \in T$. The parameter space T is usually the half-line $[0, +\infty[$. Alternatively, the stochastic process can be thought as the function $\boldsymbol{X}_t : \Omega \times T \mapsto \mathbb{R}^d$. The vector valued functions $\boldsymbol{a} : \mathbb{R}^d \mapsto \mathbb{R}^d$, $\boldsymbol{B} : \mathbb{R}^d \mapsto \mathbb{R}^d$, called the drift and the diffusion, respectively, are measurable functions satisfying a global Lipschitz and a linear growth conditions, to ensure the existence and uniqueness solution theorem [15]. If the function $\boldsymbol{B}(\boldsymbol{X}_t)$ is constant, then noise is said to be un-modulated or additive, otherwise it is said to be modulated or multiplicative.

For numerical simulations, it is often convenient to work with a-dimensional variables and time scaled equations. In the special case of a nonlinear piezoelectric energy harvester, the d-dimensional system of SDEs can be recast in the form (see section 4):

$$d\boldsymbol{X}_t = (\boldsymbol{A}\,\boldsymbol{X}_t + \boldsymbol{n}(\boldsymbol{X}_t))\,dt + \boldsymbol{B}\,dW_t \tag{10}$$

[3] We adopt the standard notation used in probability: Capital letters denote random variables, lower case letters denote their possible values.

where the constant matrix $\boldsymbol{A} \in \mathbb{R}^{d,d}$ and the function $\boldsymbol{n} : \mathbb{R}^d \mapsto \mathbb{R}^d$ collect linear and nonlinear terms of the drift, respectively, and the diffusion matrix is assumed to be constant (un-modulated noise). A-dimensional equations are obtained as a special case of linear transformed variables $\boldsymbol{y} = \boldsymbol{P}\boldsymbol{x}$, where the matrix $\boldsymbol{P} \in \mathbb{R}^{d,d}$ is a constant matrix. In order for the transformation to be invertible, $\boldsymbol{P}$ must be regular. The new variables are stochastic processes with differential

$$d\boldsymbol{Y}_t = \left(\boldsymbol{P}\boldsymbol{A}\boldsymbol{P}^{-1}\boldsymbol{Y}_t + \boldsymbol{P}\boldsymbol{n}(\boldsymbol{P}^{-1}\boldsymbol{Y}_t)\right) dt + \boldsymbol{P}\,\boldsymbol{B}\, dW_t \tag{11}$$

Linear time scaling is obtained introducing in equation (11) the time transformation $t \to t' = \tau(t) = t/T$, that implies $dt = Tdt'$. Using the change of time theorem for Itô integrals (see [15], page 156) the time scaled Wiener process is

$$W_{\tau(t)} = \sqrt{\tau'(t)}\, W_t = \frac{1}{\sqrt{T}}\, W_t \tag{12}$$

with differential

$$dW_t = \sqrt{T}\, dW_{t'} \tag{13}$$

Finally the SDEs for the transformed variables with time scaling is

$$d\boldsymbol{Y}_{t'} = T\, \left(\boldsymbol{P}\boldsymbol{A}\boldsymbol{P}^{-1}\boldsymbol{Y}_{t'} + \boldsymbol{P}\boldsymbol{n}(\boldsymbol{P}^{-1}\boldsymbol{Y}_{t'}\right) dt' + \sqrt{T}\, \boldsymbol{P}\,\boldsymbol{B}\, dW_{t'} \tag{14}$$

4 Nonlinear piezoelectric energy harvesting: Stochastic model analysis

The assumption that ambient mechanical vibrations can be modelled as white Gaussian noise, leads to substitute the external voltage source $v_{in}(t)$ in the equivalent circuit, with a stochastic voltage source $v_{in}(t)dt = D\, dW_t$, where $D > 0$ is a constant that measure the noise intensity and variance.

The system of differential equations (5) is rewritten as a system of SDEs in the form (10), with $\boldsymbol{X}_t = [q, \varphi, i, e]^T$, $\boldsymbol{n}(\boldsymbol{X}_t) = [0, -q^3/C_3, 0, 0]^T$, $\boldsymbol{B} = [0, D, 0, 0]^T$ and

$$\boldsymbol{A} = \begin{bmatrix} 0 & \frac{1}{L_1} & 0 & 0 \\ -\frac{1}{C_1} & -\frac{R_1}{L_1} & 0 & -\frac{1}{n} \\ 0 & 0 & 0 & \dfrac{1}{L} \\ 0 & \frac{1}{nC_{pz}L_1} & -\frac{1}{C_{pz}} & -\frac{G}{C_{pz}} \end{bmatrix} \tag{15}$$

The SDEs for a-dimensional variables are obtained introducing the diagonal matrix $\boldsymbol{P} = \mathrm{diag}[Q^{-1}, TQ^{-1}L_1^{-1}, TQ^{-1}, C_1Q^{-1}]$, where Q is a normalization factor that has dimension of a charge, and T is the time scaling factor $T = \sqrt{L_1C_1}$.

Similarly, for the resistive load case the system of differential equations (8) can be rewritten in the form (10), with $\boldsymbol{X}_t = [q, \varphi, e]^T$, $\boldsymbol{n}(\boldsymbol{X}_t) = [0, -q^3/C_3, 0]^T$, $\boldsymbol{B} = [0, D, 0]^T$ and

$$\boldsymbol{A} = \begin{bmatrix} 0 & \frac{1}{L_1} & 0 \\ -\frac{1}{C_1} & -\frac{R_1}{L_1} & -\frac{1}{n} \\ 0 & \frac{1}{nC_{pz}L_1} & -\frac{G}{C_{pz}} \end{bmatrix} \tag{16}$$

SDEs for the a-dimensional variables are obtained using the matrix $\boldsymbol{P} = \text{diag}[Q^{-1}, TQ^{-1}L_1^{-1}, C_1Q^{-1}]$, and the time scaling factor $T = \sqrt{L_1C_1}$.

To verify whether the power factor corrected load increases the harvested power also for the white Gaussian noise case, we have performed Monte Carlo simulations on the SDEs system (14), for both the resistive-inductive and the resistive loads. The SDEs have been solved numerically using various numerical integration schemes: Euler-Maruyama, strong order 1 stochastic Runge–Kutta, and weak order 2 stochastic Runge–Kutta [18]. Time simulation length was $\Delta t = 10^4$s, with a constant time integration step $\delta t \approx 30\mu$s. Given the relatively small time step, different numerical schemes do not show significant differences between each other. Expected values were calculated averaging over 100 different realizations of the Wiener process W_t. In our simulations, we used values of the circuit components taken from [17], and summarized in table 1. For the nonlinearity, we assumed $C_3 = Q^2 \cdot C_1$, where $Q = 1$C.

Parameter	**Value**
R_1	6.9366 Ω
C_1	5.874 μF
L_1	1 H
C_{pz}	80.08 nF
R	1 MΩ
n	37.4254
D	10 mV

Table 1. Values of circuit components, based on [17]

Figure 4 shows the root mean square values for the current $i_{rms} = \sqrt{\langle i^2(t) \rangle}$ and the output voltage $e_{rms} = \sqrt{\langle e^2(t) \rangle}$, versus the value of the inductance L, for the resistive-inductive load case. The output voltage has a maximum at $L = 73.3934$ H. We stress that the high value of the optimum inductance is a consequence of the fact that inductance L_1 is normalized to 1H. The maximum value for the output voltage is $e^{max}_{RL,rms} = 5.6423$V. By comparison, for the same values of the components, the resistive load offers a maximum output voltage $e^{max}_{RL,rms} = 2.0263$V.

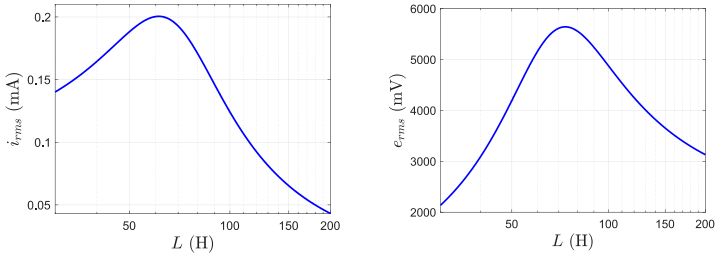

Fig. 4. Root mean square values for the current i (left) and the output voltage e (right) versus the value of the inductance L, for the resistive-inductive load.

The average power absorbed by the load is

$$P_{out} = G\, e_{rms}^2 \tag{17}$$

Figure 5 shows the output average power versus the value of the inductance. Obviously, the maximum output average power and maximum output voltage are achieved for the same value of the inductance L. Again, the resistive-inductive load offers a much higher output power with respect to the simple resistive load.

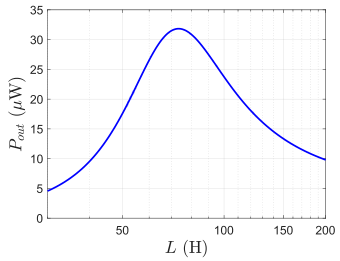

Fig. 5. Output average power versus the value of the inductance L, for the resistive-inductive load.

To determine the power efficiency, the average power injected into the system by the noise is needed. Tellegen's theorem implies that the only elements absorbing average power in the equivalent circuit of figure 3 are the resistors R_1 and R. Using the constitutive relationship for the inductor: L_1 implies $\dot{q} = \varphi/L_1$, we have that the input average power is

$$P_{in} = \frac{R_1}{L_1^2}\, \varphi_{rms}^2 + G\, e_{rms}^2 \tag{18}$$

where $\varphi_{rms} = \sqrt{\langle \varphi^2 \rangle}$. The power efficiency is then given by $\varepsilon = P_{out}/P_{in}\%$. Table 2 summarizes the main results for both a resistive load and a resistive-inductive load. The latter solution offers better performances in all aspect. In

particular, the output voltage is increased by almost three times, while the output power and power efficiency are increased by almost eight times.

Load	e_{rms}^{max}	P_{out}	ε
Resistive	2.0263 V	4.1059 μW	8.217%
Resistive-inductive	5.6423 V	31.835 μW	63.67 %

Table 2. Performances comparison for a simple resistive load, and a resistive-inductive load, with $L = 73.3634$H.

Finally, figure 6 shows the asymptotic marginal probability distribution for the output voltage $p_{st}(e) = \lim_{t \to +\infty} p(e,t)$. The probability to find a voltage value in the interval $e + de$ is evaluated as the fraction of samples falling in such an interval, normalized to the total number of samples. The stationary distribution for the resistive load (on the left) is compared to the one the resistive-inductive load (on the right). Positioning the inductor in parallel with the resistor, the variance of the output voltage is increased, as it can be clearly seen from the stationary distributions (note the different x-scales).

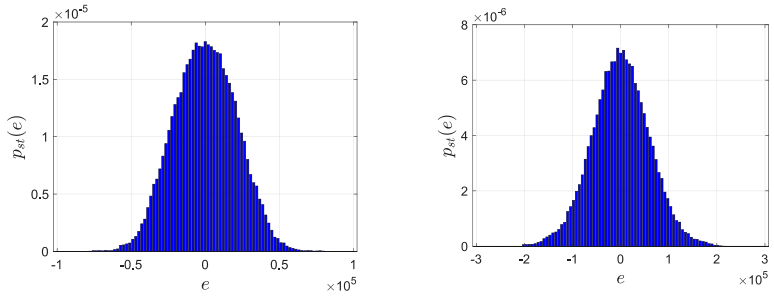

Fig. 6. Marginal stationary probability distribution for the output voltage. Resistive load (left) and resistive-inductive load(right). Value of the inductance is $L = 73.3934$H.

5 Conclusions

Piezoelectric energy harvesters are micro-electro-mechanical systems, that are capable to convert ambient mechanical vibrations into usable electrical energy. They can be used as a power source for electronic circuits, sensors and actuators, and are particularly well suited to supply power to wireless networks of sensors and actuators.

The most important limiting key factor for vibrational energy harvesting is the impedance mismatch between the mechanical and the electrical parts.

A possible solution is to use power factor correction method of circuit theory. Positioning a reactive element in parallel with the load, the lag between the voltage and current through the load can be reduced, thereby increasing the absorbed power.

In this work we analyzed a piezoelectric energy harvester for ambient mechanical vibrations. The equations of motion have been derived from the mechanical properties, the characterization of piezoelectric materials and the electrical circuit description of the load. In the case of random ambient vibrations described as white Gaussian noise, the resulting stochastic differential equations have been solved numerically, and expected quantities have been calculated using Monte-Carlo methods.

Our analysis shows that the power factor corrected solution offer better performances in terms of output voltage, output average absorbed power and power efficiency. The output voltage is increased by almost three times, while absorbed power and power efficiency are increased by almost eight times.

References

1. Roundy, S., Wright, P.K., Rabaey, J.M.: Energy Scavenging for Wireless Sensor Networks; Springer: Boston, MA, USA, (2003).
2. Paradiso, J.A., Starner, T.: Energy scavenging for mobile and wireless electronics. IEEE Pervasive Comput., 4:18–27, (2005).
3. Beeby, S.P., Tudor, M.J., White, N.: Energy harvesting vibration sources for microsystems applications. Meas. Sci. Technol. 17:R175 (2006)
4. Mitcheson, P., Yeatman, E., Rao, G., Holmes, A., Green, T.: Energy Harvesting From Human and Machine Motion for Wireless Electronic Devices. Proc. IEEE, 96:1457-1486. (2008).
5. Lu, X., Wang, P., Niyato, D., Kim, D.I., Han, Z. Wireless Networks With RF Energy Harvesting: A Contemporary Survey. IEEE Commun. Surv. Tutor., 17, 757-789 (2015).
6. Khaligh, A., Zeng, P., Zheng, C. Kinetic energy harvesting using piezoelectric and electromagnetic technologiesstate of the art. IEEE Trans. Ind. Electron., 57:850860 (2009).
7. Vocca, H., Neri, I., Travasso, F., Gammaitoni, L. Kinetic energy harvesting with bistable oscillators. Appl. Energy , 97:771776 (2012).
8. Wen, X., Yang, W., Jing, Q., Wang, Z.L. Harvesting broadband kinetic impact energy from mechanical triggering/vibration and water waves. ACS Nano, 8, 74057412 (2014)
9. Fu, Y., Ouyang, H., Davis, R.B. Nonlinear dynamics and triboelectric energy harvesting from a three-degree-of-freedom vibro-impact oscillator. Nonlinear Dyn., 92:19852004 (2018).
10. Bonnin, M., Traversa, F.L., Bonani F.: Leveraging circuit theory and nonlinear dynamics for the efficiency improvement of energy harvesting. Nonlinear Dyn. 104:367–382 (2021).
11. Daqaq, M.F. Response of uni-modal Duffing-type harvesters to random forced excitations. J. Sound Vib., 329:36213631 (2010).
12. Bonnin, M., Traversa, F.L., Bonani F.: Analysis of influence of nonlinearities and noise correlation time in a single-DOF energy-harvesting system via power balance description. Nonlinear Dyn. 100:119–133 (2020).

13. Huang, D., Zhou, S., Litak, G.: Analytical analysis of the vibrational tristable energy harvester with a RL resonant circuit. Nonlinear Dyn. 97:663677 (2019).
14. Bonnin, M., Traversa, F.L., Bonani F.: An Impedance Matching Solution to Increase the Harvested Power and Efficiency of Nonlinear Piezoelectric Energy Harvesters. Energies, 15:2764 (2022).
15. Øksendal, B.: Stochastic differential equations. Springer, Berlin, Heidelberg, (2003).
16. Priya, S., Inman, D.J.: Energy Harvesting Technologies. Springer: Boston, MA, USA, Volume 21, (2009)
17. Yang, Y. and Tang, L.: Equivalent circuit modeling of piezoelectric energy harvesters. J INTEL MAT SYST STR, 20(18): 2223–2235 (2009)
18. Särkkä S., Solin A.: Applied Stochastic Differential Equations. Cambridge University Press, Volume 10, (2019)